Electronic Supplementary Information

A facile and rapid approach to synthesize uric acid-capped Ti$_3$C$_2$ MXene quantum dots for the sensitive determination of 2,4,6-trinitrophenol both on surfaces and in solution

Xin Wang[a], Xiaodan Zhang[a], Haiyan Cao[b]*, Yuming Huang[a]*

[a]*Key Laboratory of Luminescence Analysis and Molecular Sensing (Southwest University), Ministry of Education, College of Chemistry and Chemical Engineering, Southwest University, Chongqing 400715, China. E-mail: ymhuang@swu.edu.cn*

[b]*Key Laboratory of Chongqing Inorganic Special Functional Materials, College of Chemistry and Chemical Engineering, Yangtze Normal University, Chongqing 408100, China. E-mail: caohaiyan@yznu.edu.cn*

Optimizing experimental conditions for TNP determination

For the purpose of detecting TNP accurately, we investigated the effects of pH and dilution factor on the determination of TNP. As shown in Fig. S6A, when the UA@Ti$_3$C$_2$ QDs were diluted at different multiples, the fluorescence intensity was unchanged basically. The mixture of UA@Ti$_3$C$_2$ QDs and TNP was adjusted to different pH values by HCl and NaOH, and the fluorescence intensity did not change significantly (Fig. S6B). The two figures proved that the effect of dilution factor and pH on UA@Ti$_3$C$_2$ QDs can be ignored. In the subsequent experiments, the experimental conditions were selected as dilution by 50 times and pH 9.0. After TNP was added into UA@Ti$_3$C$_2$ QDs, the final reaction time was 5 min for maintaining the stability of the reaction system. To sum up, the optimal conditions are: (a) A 50-fold dilution of UA@Ti$_3$C$_2$ QDs; (b) a reaction time of 5 min; and (c) pH value of 9.0.

Table S1 The inner filter effect (IFE) of TNP on the fluorescence of UA@Ti$_3$C$_2$ QDs.

TNP (μM)	A_{ex}	A_{em}	CF (Corrected Factor)	I_{obsd}	I_{cor}
0	0.0110	0.0010	1.02	3137	3199.7
1	0.0275	0.0085	1.04	3056	3178.2
5	0.0620	0.0277	1.10	2876	3163.6
10	0.1145	0.0547	1.20	2626	3151.2
20	0.2205	0.1105	1.43	2082	2977.3
30	0.3375	0.1725	1.72	1641	2822.5
40	0.4433	0.2277	2.02	1268	2561.4
50	0.5345	0.2740	2.30	1081	2486.3

Table S2 Result of TNP determination in real water samples using UA@Ti$_3$C$_2$ QDs based fluorescence assay.

Sample	Added (μM)	Found (μM)[a]	Recovery (%)	RSD (%)
	0.10	0.1045	104.50	0.71
Lake water	1.00	0.9390	93.90	5.66
	5.00	4.9620	99.27	2.83
	0.10	0.1190	97.40	2.12
Tap water	1.00	0.9390	93.90	0.71
	5.00	5.0040	100.80	1.20

Table S3 Detection of spiked TNP in lake or tap water samples using UA@Ti$_3$C$_2$ QDs fluorescence method, riboflavin-based fluorescence method and thiourea dioxide-based colorimetric assay.

| Sample	Added (μM)	UA@Ti$_3$C$_2$ QDs-based FL method		Riboflavin-based FL method (μM ± SD, n=3)	Colorimetric method (μM ± SD, n=3)
		Found (μM ± SD, n=11)	RSD (%, n=11)		
Lake water	2.5	2.36 ± 0.014	0.59	2.48 ± 0.20	2.21 ± 0.31
	5.0	5.37 ± 0.006	0.11	5.59 ± 0.50	5.44 ± 0.44
	10.0	10.32 ± 0.021	0.20	9.01 ± 0.80	9.74 ± 0.76
	20.0	21.10 ± 0.006	0.03	20.36 ± 0.30	20.49 ± 0.31
	30.0	29.86 ± 0.004	0.01	33.90 ± 0.40	29.63 ± 0.44
	40.0	36.44 ± 0.005	0.01	40.86 ± 0.50	40.38 ± 0.62
Tap water	2.5	2.32 ± 0.010	0.43	2.42 ± 0.40	2.48 ± 0.31
	5.0	5.23 ± 0.009	0.17	5.10 ± 0.50	5.44 ± 0.51
	10.0	10.75 ± 0.010	0.09	10.11 ± 1.00	10.27 ± 0.38
	20.0	20.91 ± 0.008	0.04	17.90 ± 0.10	20.49 ± 0.82
	30.0	29.74 ± 0.008	0.03	28.93 ± 1.80	29.09 ± 1.52
	40.0	37.73 ± 0.012	0.03	39.84 ± 1.50	38.23 ± 0.01
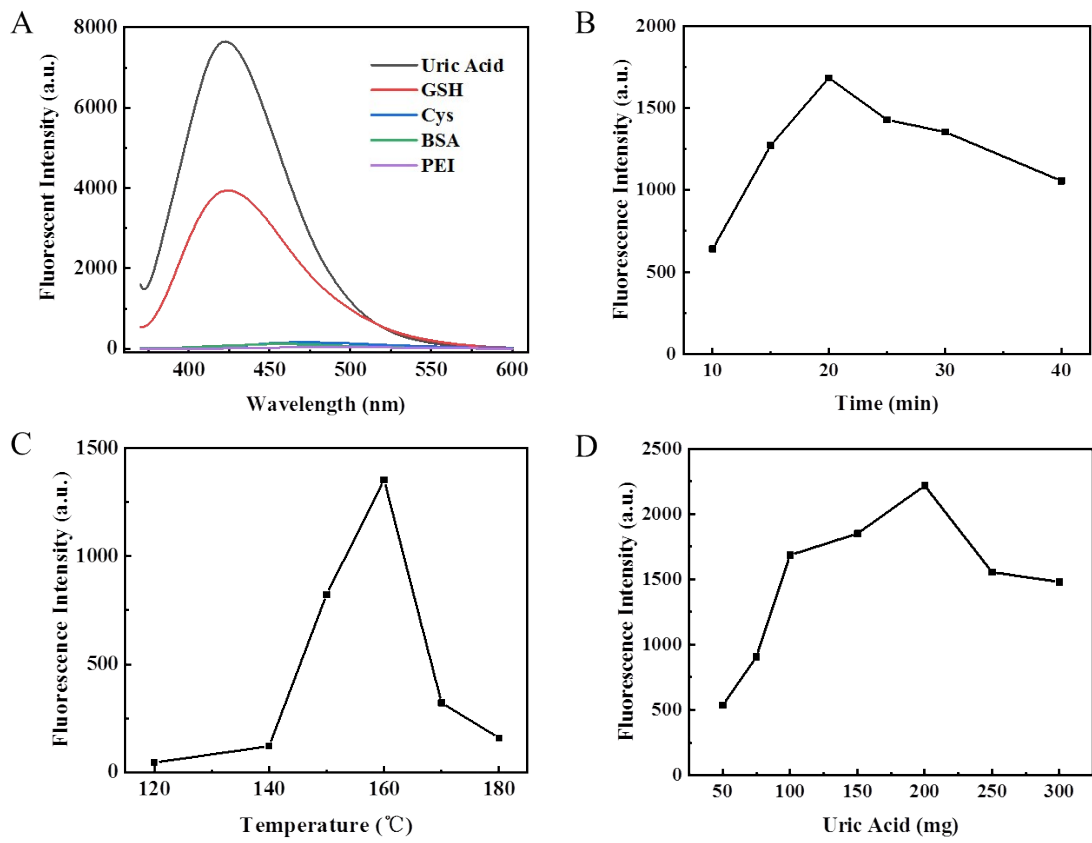
Figure S1 (A) Nitrogen sources were optimized for the synthesis of Ti_3C_2 QDs with strong fluorescence. (B) The effect of reaction time on the synthesis of $UA@Ti_3C_2$ QDs. (C) The effect of reaction temperature on the synthesis of $UA@Ti_3C_2$ QDs. (D) The effect of UA dose on the synthesis of $UA@Ti_3C_2$ QDs.
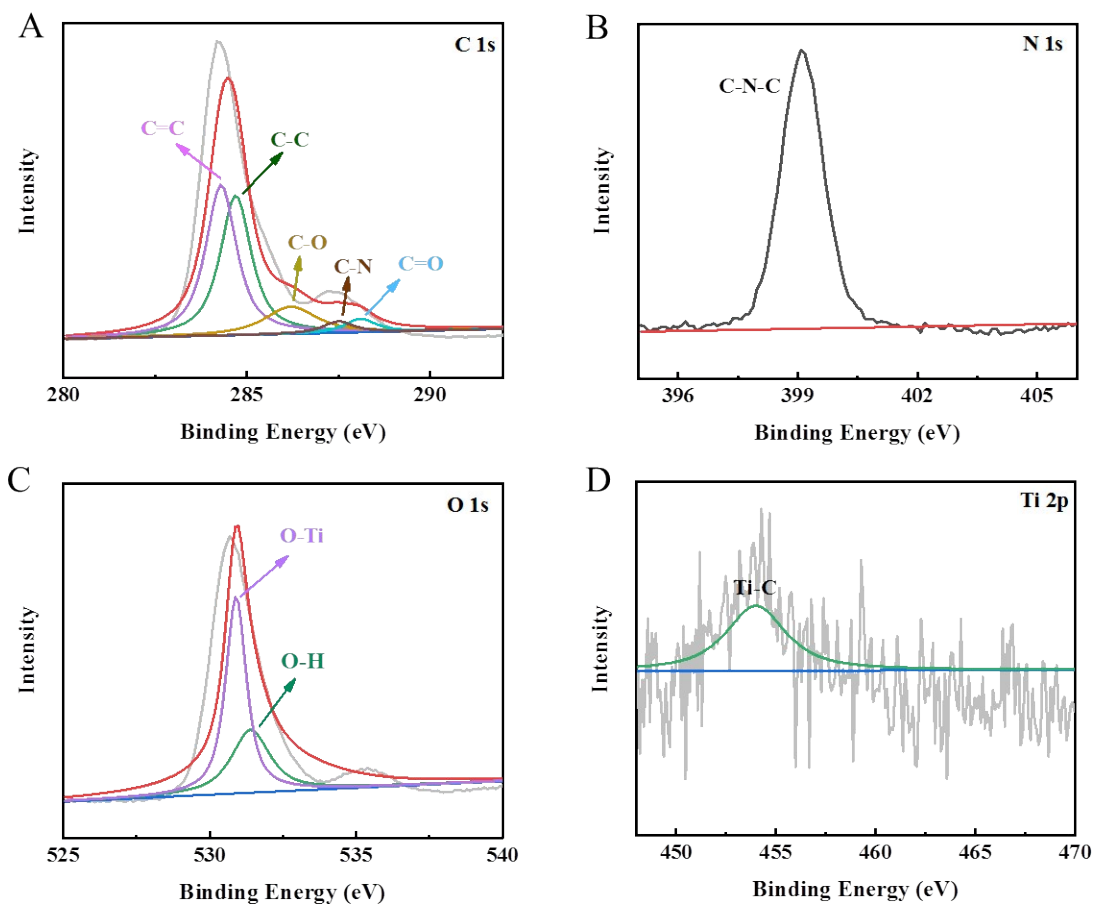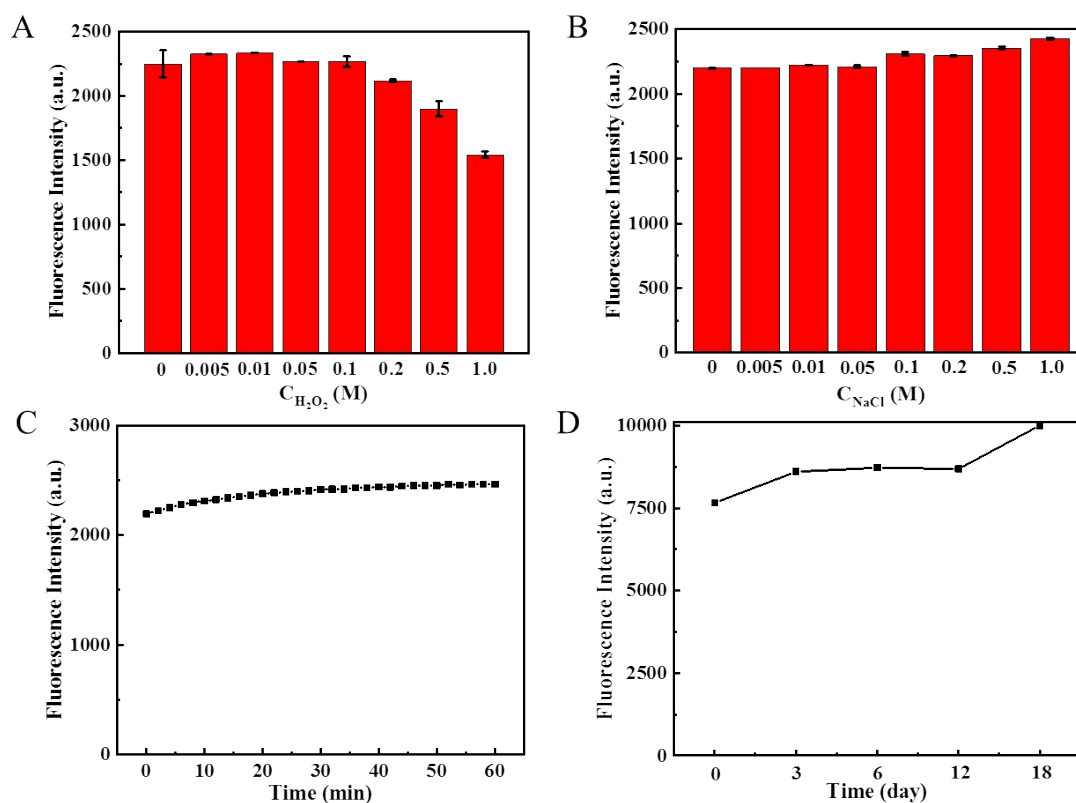
Figure S2 The narrow scan spectra of C 1s (A), N 1s (B), O 1s (C), Ti 2p (D), respectively.
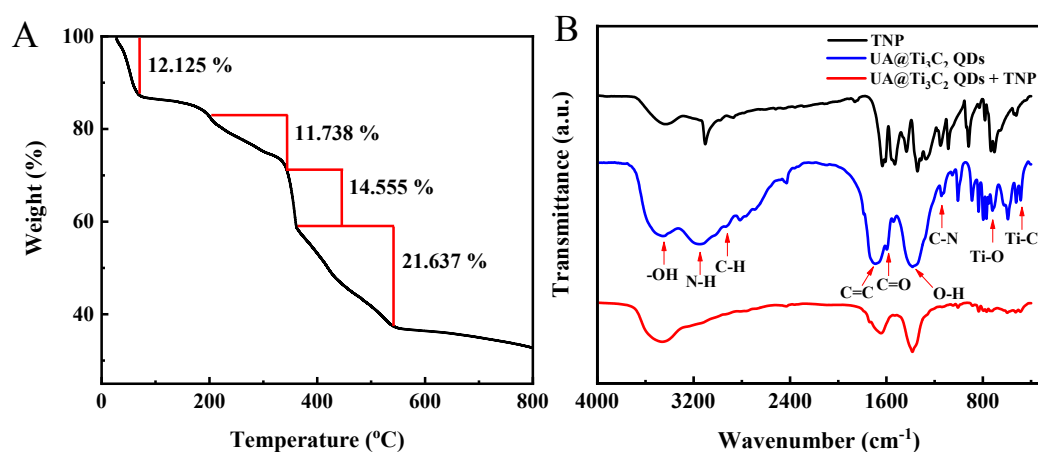

Figure S3 (A) TGA curve for the UA@Ti$_3$C$_2$ QDs. (B) FTIR spectra of TNP, UA@Ti$_3$C$_2$ QDs and UA@Ti$_3$C$_2$ QDs + TNP, respectively.
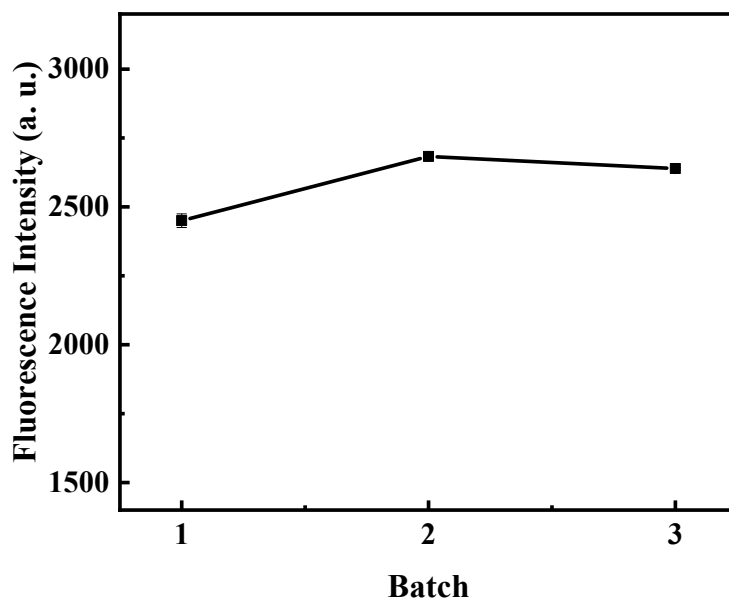
Figure S4 Differences in fluorescence intensity between three batches of UA@Ti$_3$C$_2$ QDs. The error bars represent standard deviations based on three independent measurements.

Figure S5 (A) The oxidation resistance of UA@Ti$_3$C$_2$ QDs. (B) The salt stability of UA@Ti$_3$C$_2$ QDs. (C) The photobleaching stability of UA@Ti$_3$C$_2$ QDs. (D) The storage stability of UA@Ti$_3$C$_2$ QDs. The error bars represent standard deviations based on three independent measurements.
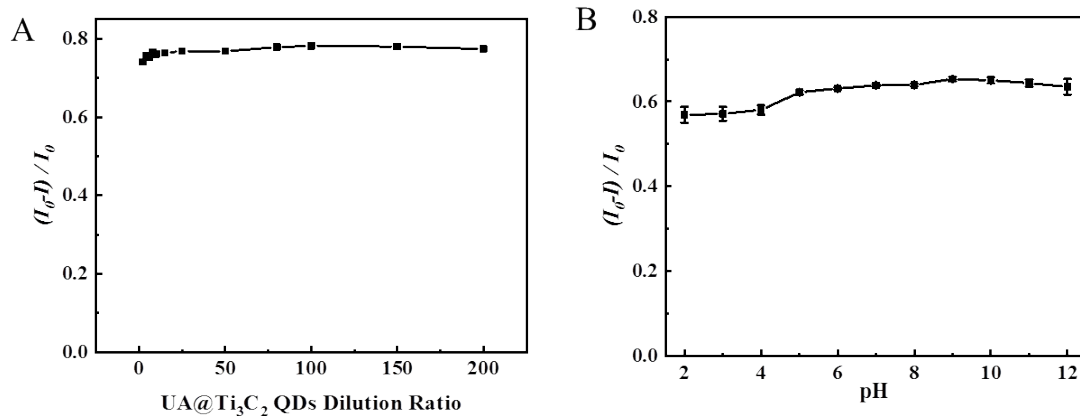
Figure S6 (A) The effect of different dilution ratios on the relative fluorescence [$(I_0-I)/I_0$ of the system; (B) The effect of pH on the relative fluorescence [$(I_0-I)/I_0$ of the system. I_0 stands the fluorescence intensity of UA@Ti$_3$C$_2$ QDs without TNP and I stands the fluorescence intensity of UA@Ti$_3$C$_2$ QDs with 50 μM TNP. The error bars represent standard deviations based on three independent measurements.
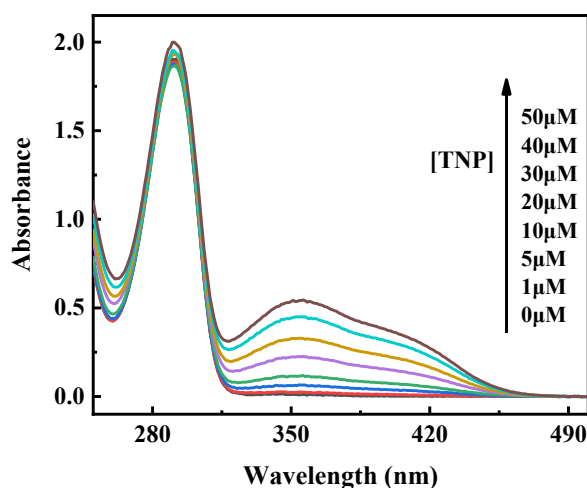

Figure S7 UV−vis absorption spectra of the UA@Ti$_3$C$_2$ QDs in the presence of different concentrations of TNP.
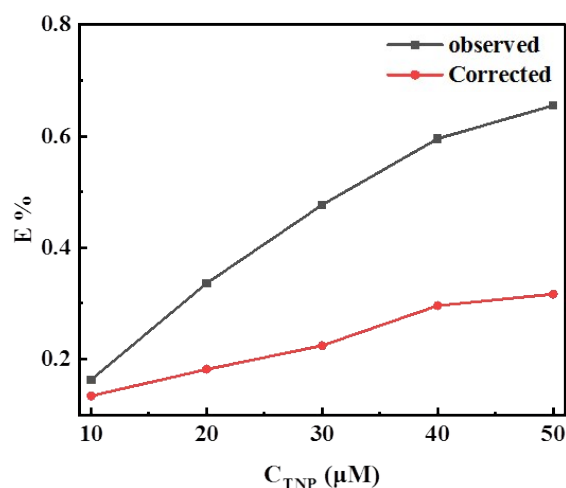
Figure S8 Suppressed efficiency (E%) of observed (black curve) and corrected (red curve) measurements for UA@Ti$_3$C$_2$ QDs after each addition of different concentrations of TNP. $E = 1 - I/I_0$. I_0 and I are the steady-state fluorescence intensities of UA@Ti$_3$C$_2$ QDs in the absence and presence of TNP, respectively.
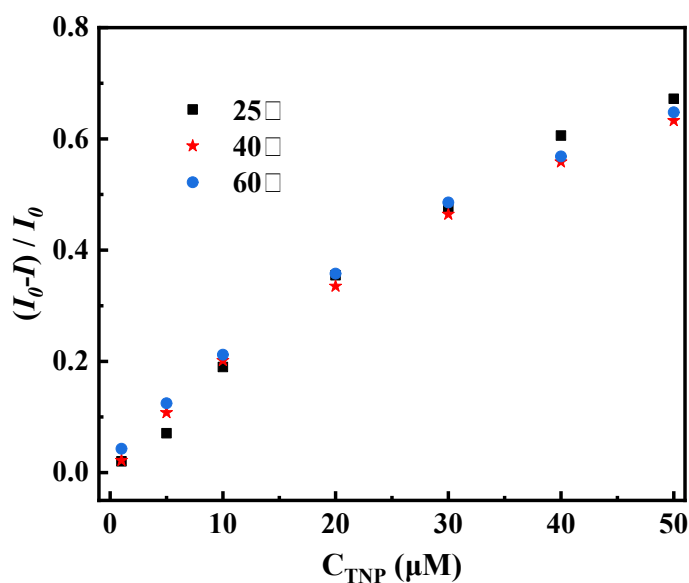
Figure S9 The effect of different temperatures on the relative fluorescence intensity $[(I_0 - I) / I_0]$ with TNP addition. I_0 and I are the fluorescence intensities of UA@Ti$_3$C$_2$ QDs in the absence and presence of TNP, respectively.